Eigenmode Structure in Solar-Wind Langmuir Waves

R. E. Ergun,[1,2] D. M. Malaspina,[2] Iver H. Cairns,[3] M. V. Goldman,[4] D. L. Newman,[4] P. A. Robinson,[3] S. Eriksson,[2] J. L. Bougeret,[5] C. Briand,[5] S. D. Bale,[6] C. A. Cattell,[7] P. J. Kellogg,[7] and M. L. Kaiser[8]

[1]*Department of Astrophysical and Planetary Sciences, University of Colorado, Boulder, Colorado 80309, USA*
[2]*Laboratory for Atmospheric and Space Physics, University of Colorado, Boulder, Colorado 80309, USA*
[3]*School of Physics, University of Sydney, Sydney, New South Wales 2006, Australia*
[4]*Center for Integrated Plasma Studies, University of Colorado, Boulder, Colorado 80309, USA*
[5]*LESIA, Observatoire de Paris, CNRS, UPMC, Université Paris Diderot, 92190 Meudon, France*
[6]*Space Sciences Laboratory, University of California, Berkeley, California, 94720, USA*
[7]*Department of Physics and Astronomy, University of Minnesota, Minneapolis, Minnesota 55455, USA*
[8]*NASA Goddard Space Flight Center, Greenbelt, Maryland, USA*

(Received 7 December 2007; published 29 July 2008)

We show that observed spatial- and frequency-domain signatures of intense solar-wind Langmuir waves can be described as eigenmodes trapped in a parabolic density well. Measured solar-wind electric field spectra and waveforms are compared with 1D linear solutions and, in many cases, can be represented by 1–3 low-order eigenstates. To our knowledge, this report is the first observational confirmation of Langmuir eigenmodes in space. These results suggest that linear eigenmodes may be the starting point of the nonlinear evolution, critical for producing solar type II and type III radio bursts.

DOI: 10.1103/PhysRevLett.101.051101 PACS numbers: 96.50.Ci, 52.25.Os, 52.35.Fp, 52.35.Mw

An understanding and physical description of the growth, evolution, and mode conversion of Langmuir waves associated with solar type II and type III radio bursts has been a topic of intense research over the past five decades [1–5]. This important astrophysical process produces intense radio emissions from the Sun, involves Langmuir wave growth in a strongly inhomogenous medium [6,7], and nonlinear evolution [8–10]. Similar complex interactions of Langmuir waves also have been studied in laboratory experiments (e.g., [11]).

Langmuir waves that produce solar type III radio bursts result from a beam-plasma instability with impulsively accelerated electrons, often from solar flares [1,2]. The electrons associated with solar type II radio bursts are believed to be shock accelerated [12]. An unstable electron distribution is produced and maintained through velocity dispersion, whereby the higher energy electron fluxes race ahead of the lower energy fluxes creating a transient bump-on-tail. The unstable electrons generate Langmuir waves which, in turn, produce electromagnetic emissions near the local electron plasma frequency and its second harmonic [8–10].

Some of the most intense Langmuir waves in the solar wind are observed as localized emissions, $O(10^3)$ Debye lengths, called ILS (intense Langmuir soliton) events [10,13]. We concentrate our study on these events. Thejappa *et al.* [10] argued that ILS events were suggestive of collapse [14], but a subsequent statistical analysis [13] found collapse, and many other localization processes, unlikely. Motivated by observations of fine frequency structure in Langmuir waves in the auroral ionosphere [15] suggesting eigenmode formation [16,17], we investigate eigenmode formation in the solar wind and show that measured ILS waveforms and their spectra are consistent with 1D linear eigenmodes of a parabolic density cavity, supporting the conclusions of laboratory experiments [11,18]. These results suggest that ambient density perturbations [19,20] can regulate the solar type III and type II source regions [21,22].

The calculation of linear eigenmodes begins with preexisting density perturbations. Strong density fluctuations are ubiquitous in the solar wind [20,21] and the majority of ILS events have peak amplitudes (E) such that $W = \varepsilon_o E^2/2nk_BT_e < 10^{-3}$ (n is density and T_e is electron temperature), suggesting the localization problem may be linear. Furthermore, nonlinear treatments have assumed linear eigenmodes as an initial condition [18,23].

For tractability, we expand the local density $n = n_o + \delta n$ to second order as a parabolic well moving at a speed (ν_n):

$$\delta n(x, t) = \tfrac{1}{2} n_o \kappa_o^2 (x - \nu_n t)^2, \tag{1}$$

where n_o is the background electron density and κ_o represents the curvature of the density perturbation. This expansion can be justified *a posteriori*.

In a frame moving at a constant speed (ν_n), δn is independent of t. Equation (1) simplifies to $\delta n = n_o \kappa_o^2 x^2/2$. The high-frequency component of the Zakharov equations [17] describes the reaction of a slowly varying envelope of a Langmuir wave, $\tilde{E}$ with $E(x, t) = \tilde{E}(x, t)e^{i(kx-\omega t)}$ constrained by $\omega^2 = \omega_p^2 + 3\nu_e^2 k^2$ to a density perturbation:

$$i\left(\frac{\partial}{\partial t} + \nu_d \frac{\partial}{\partial x}\right)\tilde{E} + \frac{3}{2}\frac{\nu_e^2}{\omega_p}\frac{\partial^2}{\partial x^2}\tilde{E} = \frac{\omega_p \delta n}{2n_o}\tilde{E}, \tag{2}$$

where ω_p is the electron plasma frequency, $\nu_e = \sqrt{T_e/m}$ (m is the electron mass), and $\nu_d = \nu_g - \nu_n$ is the difference between the Langmuir wave group velocity and the speed of the density perturbation. Since we assume that δn

preexists, the Zakharov equation describing the low-frequency response is not needed, but must be used to describe subsequent nonlinear evolution.

Following previous works [18], a solution can be found by assuming a form $\tilde{E} = A(x)e^{i(\Delta kx - \Delta\omega t)}$, where $A(x)$ is real, $\Delta\omega$ is a frequency shift, and Δk is a shift in wave number. Substitution of the above form into Eq. (2) allows for separation into real and imaginary parts:

$$\frac{3}{2}\frac{\nu_e^2}{\omega_p}\frac{\partial^2 A}{\partial x^2} = A(\Delta k\nu_d - \Delta\omega) + \frac{\omega_p \delta n}{2n_o}A + \frac{3}{2}\frac{\nu_e^2}{\omega_p}\Delta k^2 A, \tag{3}$$

$$3\Delta k\frac{\nu_e^2}{\omega_p}\frac{\partial A}{\partial x} = -\nu_d\frac{\partial A}{\partial x}. \tag{4}$$

The imaginary part [Eq. (4)] leads to $\Delta k = -\omega_p\nu_d/3\nu_e^2$. With Δk defined, Eq. (3) combines with Eq. (1) to become

$$\frac{\partial^2 A}{\partial x^2} = (Q^4x^2 - \lambda)A, \tag{5}$$

where

$$Q^4 = \frac{\omega_p^2\kappa_o^2}{6\nu_e^2} \quad \text{and} \quad \lambda = \frac{\omega_p}{3\nu_e^2}\left(2\Delta\omega + \frac{\omega_p\nu_d^2}{3\nu_e^2}\right). \tag{6}$$

Equation (5) is analogous to the Schrödinger equation and has the solution set

$$A(x) = \sum_n A_n H_n(Qx)e^{-Q^2x^2/2} \tag{7}$$

subject to the quantization condition $\lambda/Q^2 = 2n + 1$ where n is a positive integer. H_n is the nth Hermite polynomial and A_n is the amplitude of the nth mode. The full set of solutions of Langmuir eigenmodes can be expressed as

$$E(x, t) = \sum_n A_n H_n(Qx)e^{-Q^2x^2/2}e^{i(k+\Delta k)x - i(\omega+\Delta\omega_n)t}, \tag{8}$$

with the quantization rule

$$\frac{\lambda}{Q^2} = 2n + 1 \Rightarrow \Delta\omega_n = (2n + 1)\sqrt{\frac{3}{8}}\nu_e\kappa_o - \frac{\nu_d^2\omega_p}{6\nu_e^2}. \tag{9}$$

We compare these solutions to observed ILS events. The observed ILS events have not been directly associated with solar type II or type III radio bursts, but were observed during periods of solar activity. Figure 1(a) displays the electric field ($\boldsymbol{E}$) waveform of a Langmuir wave measured by the STEREO B spacecraft SWAVES instrument [24]. The STEREO spacecraft are in solar orbit at ~1 AU from the Sun. The field, $\boldsymbol{E}$, digitized at $\sim 1.25 \times 10^5$ samples per second, is derived from three orthogonal, 6-meter, cylindrical antennas mounted on the antisunward side of the spacecraft. We display events that have linear polarization (see later discussion).

Figure 1(a) shows Langmuir waves with a near-Gaussian envelope. The observed temporal envelope reflects the spatial envelope transformed by the supersonic flow of the solar wind (~400 km/s) and, to a lesser degree, the spacecraft motion. In other words, the short duration of the wave packet in Fig. 1(a) indicates spatial localization.

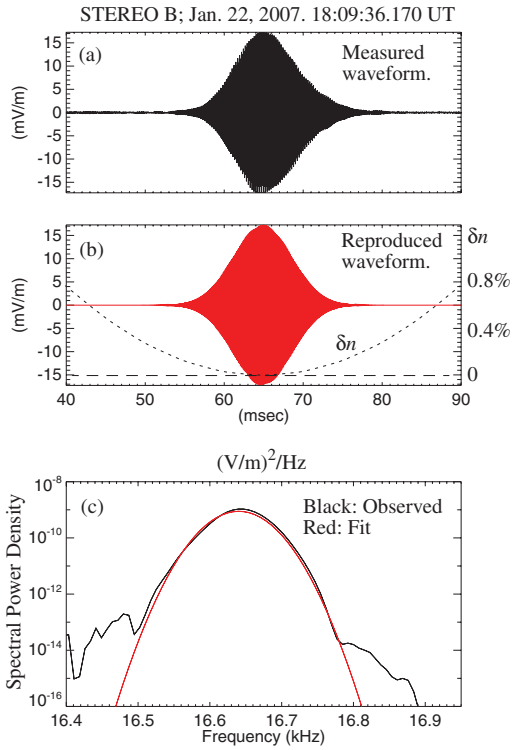

FIG. 1 (color). (a) The electric field waveform of Langmuir waves in the solar wind. The waveform has near linear polarization along $\boldsymbol{B}$. (b) The waveform reproduced from the spectral fit to Eq. (8). (c) The observed spectrum (black) and the fit to a sum of eigenmodes (red).

Figure 1(c) plots the spectral power density of the waveform (black trace). The spectrum is fit (red trace) by a sum of eigenmodes [Eq. (8)] using A_n, $Q(\kappa_o)$, ω, and k as free parameters (see Table I). The eigenmodes are in the solar-wind frame so the fit depends directly upon the solar-wind speed along the magnetic field ($\nu_{SW} \cdot \boldsymbol{B}/|\boldsymbol{B}|$) and ν_e, which are estimated from measurements made by other STEREO instruments and other spacecraft (Wind, ACE). After a spectrum is fit, the waveform is recreated by adjusting the relative phases between the eigenmodes. The recreated waveform is plotted in Fig. 1(b) along with the density structure. Electron distributions with sufficient detail to identify electron beams are not available for any of the published events.

The waveform in Fig. 1 is dominated by a single ($n = 0$) eigenmode. Figure 2 displays a more complex, but observationally more common waveform. In this event, the wave packet and spectra can be well described by the three lowest-order eigenmodes with relative amplitude fractions of 45% ($n = 0$), 50% ($n = 1$), and 5% ($n = 2$). Figure 3 displays a rare example of a highly complex waveform and spectrum. The two main lobes of the spectrum are well reproduced by a combination of modes $n = 3$ (22%), $n = 5$ (35%), $n = 7$ (26%). The side lobes require mode $n = 11$ (10%). Three other modes have low-

TABLE I. Solar wind and fitted parameters.

Event	f (kHz)	ω/k_{eff} (c)	Q^{-1} (km)	$\nu_{\mathrm{SW}} \cdot \boldsymbol{B}/\lvert\boldsymbol{B}\rvert$	T_e (eV)	k_{eff}/Q	$\varepsilon_o E^2/2nk_BT_e$
Figure 1	16.8	0.11	1.3	344 km/s	6.3	3.9	9×10^{-4}
Figure 2	22.8	0.26	4.0	279 km/s	42.5	7.4	3×10^{-4}
Figure 3	20.2	0.07	1.0	328 km/s	0.6	5.9	4×10^{-3}

level contributions including $n = 1$ (6%). All of the above fits yield very small values of curvature ($\kappa_o \ll k, Q$) such that the waveforms are confined to regions where $\delta n/n < \sim 1\%$, thus justifying the second order expansion.

Of the 1172 possible Langmuir waveforms captured by the STEREO time-domain samplers between 01 January 2007 and 31 July 2007, 204 satisfy the criteria of an isolated ILS event [10,13]. More precisely, 204 events have peak amplitudes exceeding 1 mV/m and endure for less than 130 ms. Of these 204 ILS events, 109 can be well described as a combination of the three lowest-order Hermite-Gauss functions ($n = 0, 1, 2$). The remaining 95 events require contributions from higher-order Hermite-Gauss functions ($n > 2$). Approximately 70% of the ILS events have linear polarization ($\boldsymbol{k}$ nearly along $\boldsymbol{B}$), ~20% have 2D polarization ($\boldsymbol{k}$ lies in a plane), and ~10% have more complex, 3D patterns. The 2D and 3D events may indicate linear or nonlinear mode conversion including side scatter [25] and require a multidimensional description [23].

Hermite-Gauss functions form a basis, so they can recreate any localized spatial structure or spectral shape. However, the majority of the 204 ILS events are described with the three lowest-order modes and the remaining events are often dominated by three or fewer of the higher-order modes (>95% amplitude fraction). The preponderance of the few low-order modes indicates that the Langmuir waves are in eigenstates similar to that seen in laboratory experiment [11,18].

Current instrumentation cannot measured solar-wind densities directly at needed accuracy (<1%) nor at the needed time resolution (translates to spatial resolution) to contribute to studies of ILS events. However, the frequencies of low-level Langmuir waves surrounding an ILS event suggest that they are in density cavities. Figure 4 plots an ILS event which has low-level Langmuir waves throughout the 130 ms period of the waveform capture. The frequency shift ($\delta f/f \sim 3\%$) is consistent with that required for eigenmode formation (see density curves in

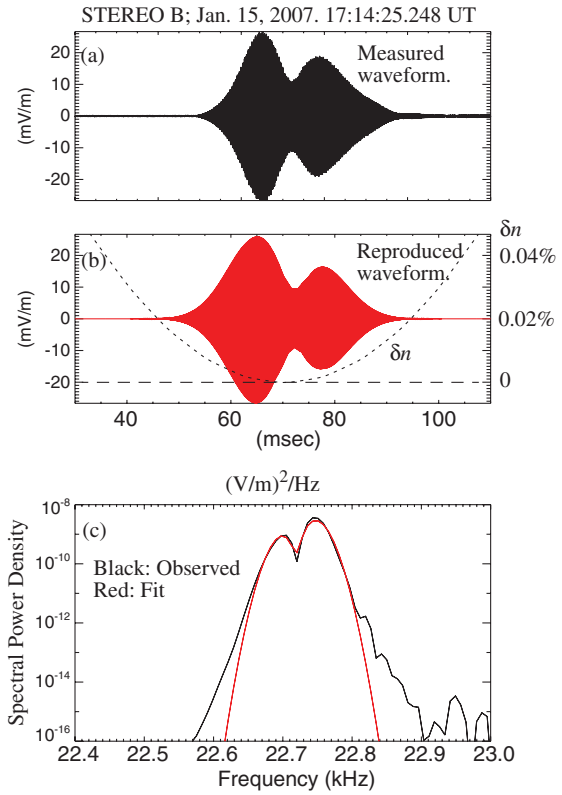

FIG. 2 (color). A more complex localized Langmuir wave event plotted in the same format as in Fig. 1. Black traces are from observations. Red traces are fits.

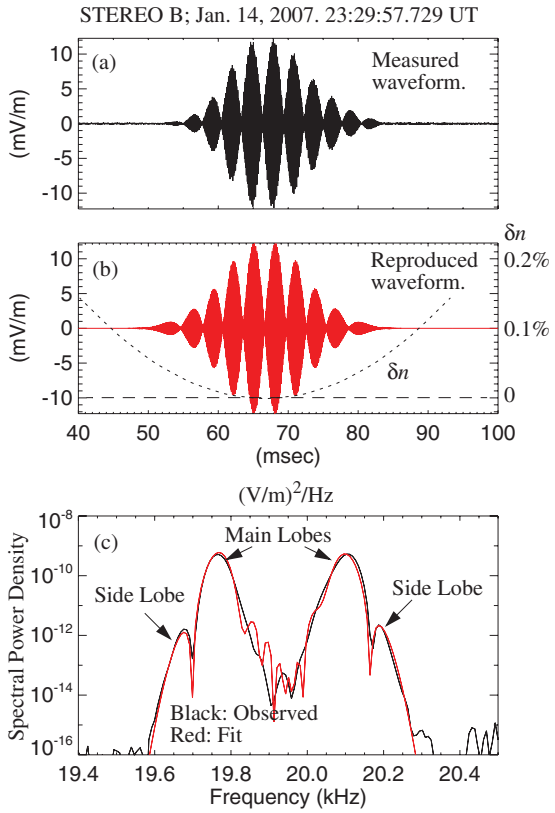

FIG. 3 (color). A highly complex localized Langmuir wave event plotted in the same format as in Fig. 1. Black traces are from observations. Red traces are fits.

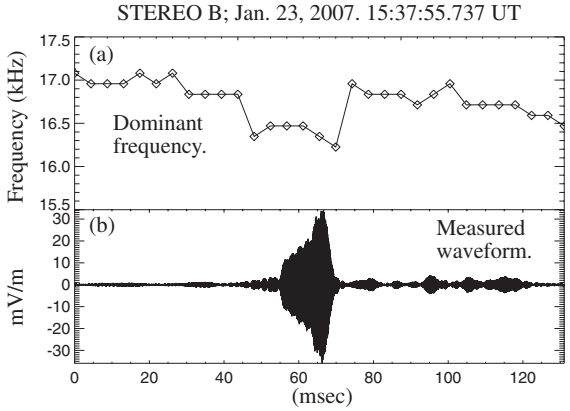

FIG. 4. (a) The dominant wave frequency of (b) the electric field waveform. The frequency of the most intense part of the wave is lower indicating trapping in a density cavity.

earlier figures). This frequency shift is far greater than spectral splitting of eigenmodes ($\Delta\omega/\omega \sim 10^{-4}$) or that from a change in the Langmuir wavelength so, if the waves are electrostatic, the frequency shift represents increased plasma density surrounding the ILS event.

These observational results open up a number of questions, particularly on the role of nonlinear processes. The majority of observed events have small peak amplitudes $\varepsilon_o E^2/2nk_BT_e < 10^{-3}$, all events analyzed so far are consistent with a large spatial extent, $O(10^3)$ Debye lengths, so a collapse process does not appear to be necessary. However, since nonlinear eigenstates (density cavity created by ponderomotive force) [26] have not been thoroughly tested against the observations, we cannot rule such effects out. The observed eigenmodes have packet sizes which contain tens of wavelengths indicating that they are not subject to strong transit-time damping [3,27] and may experience beam-driven growth. It is not clear, however, if the eigenmodes grow in place or form indirectly. If they directly grow, a saturation mechanism needs to be identified and the observation of the higher-order modes such as in Fig. 3 needs to be explained. Interestingly, our results suggest that a 1D description is adequate for most events. However, 30% of the events display complex polarization, suggesting multidimensional dynamics. The source and coherence time of the density perturbations needs to be investigated since they play a strong role in regulating the eigenstates.

In conclusion, we have demonstrated that some of the most intense Langmuir waves observed in the solar wind can be described as 1D eigenmodes localized in a parabolic density cavity [18]. The majority of the ILS events are well represented by ≤ 3 of the low-order eigenmodes, the remaining events are well described by a few higher-order eigenmodes. Furthermore, examination of the low-level Langmuir waves surrounding the ILS events support trapping in a density cavity. The localization, discrete-frequency structure, and enhanced amplitudes of the eigenmodes should make ILS events an efficient seed for fundamental and second harmonic radio wave generation. The processes that produce the electromagnetic emissions should be revisited with linear eigenmodes as a starting point.

The authors wish to thank Jack Gosling for his help and insight. This work was funded by NASA's STEREO SWAVES and by NASA's Fast Auroral Snapshot Explorer extended mission.

[1] V. L. Ginzburg and V. V. Zheleznyakov, Sov. Astron. **2**, 653 (1958).
[2] R. P. Lin *et al.*, Astrophys. J. **251**, 364 (1981).
[3] P. A. Robinson, Rev. Mod. Phys. **69**, 507 (1997).
[4] I. H. Cairns and P. A. Robinson, Astrophys. J. **509**, 471 (1998).
[5] B. Li, P. A. Robinson, and I. H. Cairns, Phys. Rev. Lett. **96**, 145005 (2006).
[6] M. V. Goldman and D. F. Dubois, Phys. Fluids **25**, 1062 (1982).
[7] B. Li, P. A. Robinson, and I. H. Cairns, Phys. Plasmas **13**, 082305 (2006).
[8] R. P. Lin, W. K. Levedahl, W. Lotko, D. A. Gurnett, and F. L. Scarf, Astrophys. J. **308**, 954 (1986).
[9] I. H. Cairns and P. A. Robinson, Geophys. Res. Lett. **19**, 2187 (1992).
[10] G. Thejappa, M. L. Goldstein, R. J. MacDowall, K. Papadopoulos, and R. G. Stone, J. Geophys. Res. **104**, 28 279 (1999).
[11] A. Y. Wong and B. H. Quon, Phys. Rev. Lett. **34**, 1499 (1975).
[12] H. V. Cane, R. G. Stone, J. Fainberg, J. L. Steinberg, S. Hoang, and R. T. Stewart, Geophys. Res. Lett. **8**, 1285 (1981).
[13] A. L. Nulsen, I. H. Cairns, and P. A. Robinson, J. Geophys. Res. **112**, 632 (2007).
[14] V. E. Zakharov, Sov. Phys. JETP **35**, 908 (1972).
[15] K. L. McAdams and J. Labelle, Geophys. Res. Lett. **26**, 1825 (1999).
[16] K. L. McAdams, R. E. Ergun, and J. Labelle, Geophys. Res. Lett. **27**, 321 (2000).
[17] P. H. Yoon and J. LaBelle, J. Geophys. Res. **110**, 308 (2005).
[18] G. J. Morales and Y. C. Yee, Phys. Fluids **19**, 690 (1976).
[19] T. W. J. Unti, M. Neugebauer, and B. E. Goldstein, Astrophys. J. **180**, 591 (1973).
[20] A. I. Efimov, *et al.*, Adv. Space Res. **36**, 1448 (2005).
[21] P. A. Robinson, Sol. Phys. **139**, 147 (1992).
[22] P. J. Kellogg, K. Goetz, S. J. Monson, and S. D. Bale, J. Geophys. Res. **104**, 17 069 (1999).
[23] H. Alinejad, P. A. Robinson, I. H. Cairns, O. Skjæraasen, and S. Sobhanian, Phys. Plasmas **14**, 072304 (2007).
[24] J. L. Bougeret *et al.*, Space Sci. Rev. (to be published).
[25] S. D. Bale, P. J. Kellogg, K. Goetz, and S. J. Monson, Geophys. Res. Lett. **25**, 9 (1998).
[26] K. Mima, K. Kato, and K. Nishikawa, J. Phys. Soc. Jpn. **42**, 290 (1977).
[27] P. A. Robinson, Phys. Fluids B **3**, 545 (1991).